frontiers | Frontiers in Earth Science

ORIGINAL RESEARCH
published: 23 May 2022
doi: 10.3389/feart.2022.915500

Investigation of Modern *n*-Alkanes in Daihai Lake Basin, Northern China: Implications for the Interpretation of Paleoclimate Research

Zhongwei Shen[1], Zhiping Zhang[1], Jie Chen[1], Lin Chen[1], Xin Pang[2], Ruijin Chen[1], Jianbao Liu[3] and Shengqian Chen[3]**

[1]Key Laboratory of Western China's Environmental Systems (Ministry of Education), College of Earth and Environmental Sciences, Lanzhou University, Lanzhou, China, [2]Daihai Nature Reserve Service Center in Liangcheng County, Ulanqab, China, [3]Group of Alpine Paleoecology and Human Adaptation (ALPHA), State Key Laboratory of Tibetan Plateau Earth System, Resources and Environment (TPESRE), Institute of Tibetan Plateau Research, Chinese Academy of Sciences, Beijing, China

OPEN ACCESS

Edited by:
Xianyong Cao,
Institute of Tibetan Plateau Research (CAS), China

Reviewed by:
Cheng Zhao,
Nanjing University, China
Jiaju Zhao,
Institute of Earth Environment (CAS), China

***Correspondence:**
Zhiping Zhang
zhangzhp12@lzu.edu.cn
Shengqian Chen
sqchen@itpcas.ac.cn

Specialty section:
This article was submitted to Quaternary Science, Geomorphology and Paleoenvironment, a section of the journal Frontiers in Earth Science

Received: 08 April 2022
Accepted: 22 April 2022
Published: 23 May 2022

Citation:
Shen Z, Zhang Z, Chen J, Chen L, Pang X, Chen R, Liu J and Chen S (2022) Investigation of Modern n-Alkanes in Daihai Lake Basin, Northern China: Implications for the Interpretation of Paleoclimate Research. Front. Earth Sci. 10:915500. doi: 10.3389/feart.2022.915500

n-Alkanes are one of the most used proxies in lake sediments to reconstruct past climate change. However, the distribution and concentration of *n*-alkanes are controlled by multiple factors, and their interpretation across northern China has revealed obvious discrepancies. It is therefore important to investigate the controlling factors of *n*-alkane proxies before using them for paleoclimate reconstruction. In this study, we collected fresh plant leaves, basin surface soils, lake surface sediments, and a short sediment core (DH20B) in the Daihai Lake basin to analyze the paleoclimate implications of *n*-alkanes. Our results show that long-chain (C_{27}–C_{35}) *n*-alkanes in Daihai Lake are dominated by allochthonous sources. The average chain length of long-chain *n*-alkanes ($ACL_{27–35}$) and total long-chain *n*-alkane concentration ($\sum alk_{long\text{-}chain}$) of DH20B are significantly correlated with regional summer temperature ($r = 0.54$, $p < 0.01$) and summer precipitation ($r = 0.41$, $p < 0.05$) over the past 60 years. These results indicate that $ACL_{27–35}$ and $\sum alk_{long\text{-}chain}$ from Daihai Lake sediments have the potential to reconstruct past summer temperature and summer precipitation, respectively, because higher summer temperature promotes the synthesis of longer-chain *n*-alkanes to reduce water loss (leading to higher $ACL_{27–35}$) and increased summer precipitation promotes plant growth (leading to higher $\sum alk_{long\text{-}chain}$). Moreover, we found that human activity significantly affected $\sum alk_{long\text{-}chain}$ through cultivation and grazing after 2005. Our findings may have broad significance for paleoclimate reconstruction of other hydrologically closed lakes, highlighting the importance of proxy validation studies.

Keywords: *n*-alkane, proxy validation study, summer precipitation, summer temperature, human activity, Daihai Lake

1 INTRODUCTION

n-Alkanes are a series of saturated straight-chain hydrocarbons (with a chemical formula of C_nH_{2n+2}) with different carbon numbers, which contain no active functional groups and are stable in natural environments (Eglinton and Hamilton, 1967). They are biosynthesized from long-chain fatty acids via the decarboxylation pathway from living organisms (Villanueva et al., 2014) and contain abundant information about biogenic sources and environmental changes (e.g., Castañeda and Schouten, 2011;

Diefendorf and Freimuth, 2017; Huang et al., 2018). Given their advantages of chemical inertness, water insolubility, and high content, *n*-alkanes in lake sediments are widely used in paleoclimate research studies (e.g., Ficken et al., 2000; Castañeda and Schouten, 2011; Bush and McInerney, 2013; Zhang et al., 2020; Zhao et al., 2021).

Northern China is the birthplace of Chinese culture and awareness of the eco-fragile area (Chen et al., 2015; Shen et al., 2018), so *n*-alkane-based paleoclimate reconstruction in this region can provide an important method to understand past human habitats and environmental change. However, the average chain length (ACL) and the total *n*-alkane concentration (∑alk)—the two most used *n*-alkane-based proxies in paleoclimate research—are controlled by multiple factors, such as temperature, precipitation, and vegetation type (Bush and McInerney, 2013; Diefendorf and Freimuth, 2017; Kou et al., 2020), and the interpretations of them across northern China has revealed obvious discrepancies (e.g., Duan et al., 2014; Wang et al., 2018). For example, ACL was suggested to be a temperature indicator in a modern *n*-alkane study based on 357 plant leaves in northern China (Wang et al., 2018), and this conclusion was applied in Xijianhaizi Lake (Dong et al., 2022) and Hani peatland (Zhou et al., 2010). However, in Tianchi Lake (Sun et al., 2018), Xiaolongwan Lake (Sun et al., 2013), and Dabusu Lake (Sawada et al., 2020), ACL was more likely to be influenced by changes in plant type. Meanwhile, Zhang et al. (2019) used ∑alk in Beilianchi Lake to indicate the productivity of the lake basin, which was linked to precipitation changes. By contrast, researchers pointed out that temperature also influenced ∑alk in Xingkai Lake, (Sun et al., 2019), a conclusion that was also supported by studies of Wang et al. (2018).

Moreover, in addition to the climate drivers, human activity is also an important factor influencing *n*-alkanes. For example, He et al. (2020) pointed out that intense human activities (e.g., fuel combustion and intensive cultivation) significantly changed the odd-to-even carbon preference and the concentration of *n*-alkanes in Chaohu Lake, southern China. However, in most modern *n*-alkane studies in northern China, research has focused on the climate factors, and the influence of human activity has not been fully considered (e.g., Duan and Xu, 2012; Duan et al., 2014; Wang et al., 2018). In summary, detailed investigations of modern *n*-alkane processes are needed before paleoclimate reconstruction is undertaken in northern China.

Daihai Lake is the fourth largest lake in Inner Mongolia and is an ideal place for paleoclimate research in northern China (e.g., Wang et al., 1990; Zheng et al., 2010; Jin et al., 2013; Xiao et al., 2019). Here, to investigate the paleoclimatic interpretations of *n*-alkanes in Daihai Lake, modern plant leaves, basin surface soils, lake surface sediments, and a lake sediment core were collected in the region. Our objectives were: 1) to investigate the source of *n*-alkanes; 2) to assess the paleoclimatic interpretation of *n*-alkanes; and (3) to evaluate the impacts of human activity on *n*-alkanes.

2 STUDY AREA

The Daihai Lake basin is situated in Inner Mongolia, northern China (**Figure 1A**), with an area of 2,263.3 km^2. It is the transition zone between semi-arid and semi-humid areas and is thus sensitive to climate change. The annual average temperature and precipitation in this region over the past 60 years are 5.9°C and 406.4 mm, respectively, with both maximums occurring in summer. The modern natural vegetation in the basin is temperate steppe, dominated by trees such as *Betula platyphylla*, *Pinus tabulaeformis*, and *Salix*, and grasses and herbs including *Stipa krylovii*, *Artemisia sacrorum*, *Medicago falcata*, and *Potentilla chinensis* as well as aquatic plants in Daihai Lake such as *Ceratophyllum demersum*, *Vallisneria natans*, and *Stuckenia pectinata* (Wang et al., 1990). Daihai Lake is a hydrologically closed lake, with a surface area of 68.67 km^2 and a maximum water depth of ~7.0 m (**Figure 1B**). The water sources of Daihai Lake are mainly fed by regional precipitation through six seasonal surface rivers (Gongba, Wuhao, Buliang, Tiancheng, Muhua, and Suodai).

Recently, human activities in the region have increased significantly, which has had a huge influence on the Daihai Lake basin. First, the land type has changed significantly, with 60% of the land area now arable and grass (Liang et al., 2021). Given the huge consumption of water for agriculture, the area of Daihai Lake has contracted sharply over the past decades (Liang et al., 2021). Second, the Daihai power plant was built on the southern shore of Daihai Lake in 2005 (Inner Mongolia Water Conservancy and Hydropower Survey and Design Institute, 2015). Since 2008, a large volume of lake water (~1.192 × 10^7 m^3 each year) has been used in the power plant to cool the facility, with the used water directly returned into Daihai Lake.

3 MATERIALS AND METHODS

3.1 Research Materials

All samples used in this study (**Supplementary Table S1**) were collected in the Daihai Lake basin in July 2020 (**Figure 1C**): 1) 19 fresh plant leaf samples (four submerged aquatic plants and 15 terrestrial plants); 2) 7 undisturbed basin surface soil (BSS) samples—to reduce the sampling error, mixed soils in the quadrat (with an area of 1 m^2) were taken; 3) 21 lake surface sediment (LSS) samples from different lake water depths; and 4) a 70-cm long sediment core (DH20B) was retrieved from the center of the lake. DH20B was sliced at 0.5 cm intervals in the field. All samples were transported to the laboratory and stored at a temperature below 4°C. Then, all samples were freeze-dried for subsequent analyses.

3.2 Dating Method

The activities of ^{137}Cs, ^{210}Pb, and ^{226}Ra of 45 samples were measured (Model GCW 3523, CANBERRA Industries Inc.) to determine the age control of DH20B (**Figure 2**). About 7 g of dry sediments were ground and packed in polyethylene tubes. Then all tubes were stored in a sealed container for 3 weeks to allow for radioactive equilibration. ^{137}Cs was measured via gamma emission at 661.6 keV, and ^{210}Pb was detected at its energy emission at 46.5 keV. ^{226}Ra was determined by measuring the gamma ray spectrum peak area of ^{214}Pb (241.9, 295.2, and

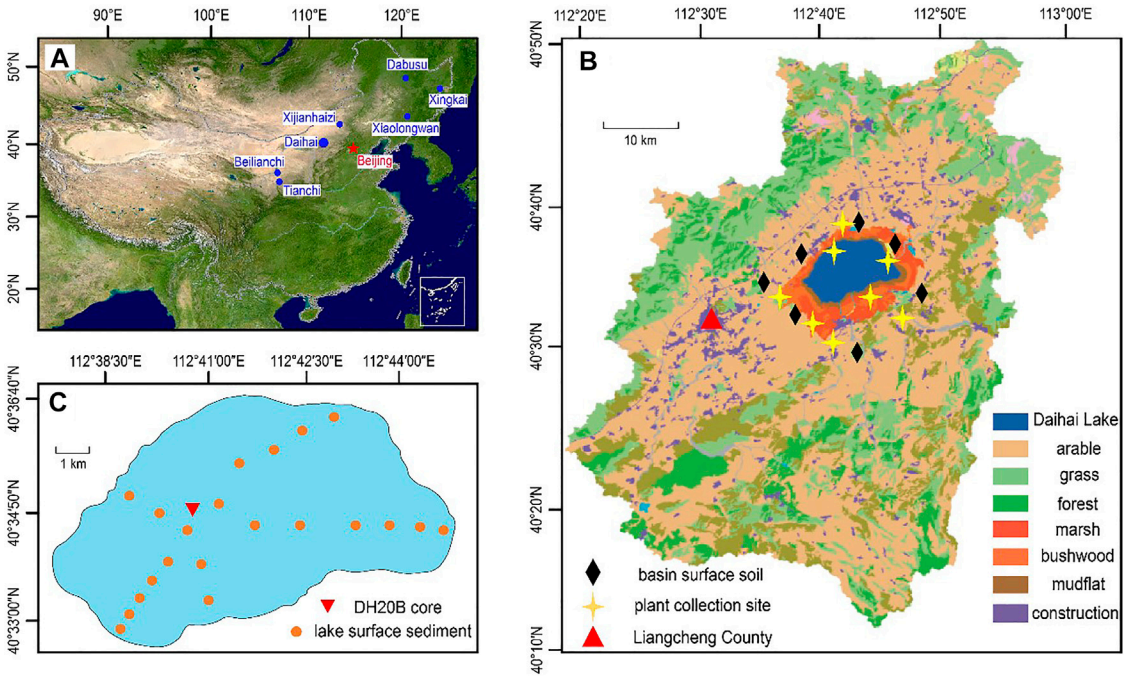

FIGURE 1 | Study site and sampling locations. **(A)** Location of Daihai Lake and other lakes cited in this study. **(B)** Map of land use in the Daihai Lake basin, modified from Liang et al. (2021). The diamonds and crosses indicate the basin soil and plant leaf sampling sites, respectively. **(C)** Daihai Lake area and sampling sites of DH20B and lake surface sediment.

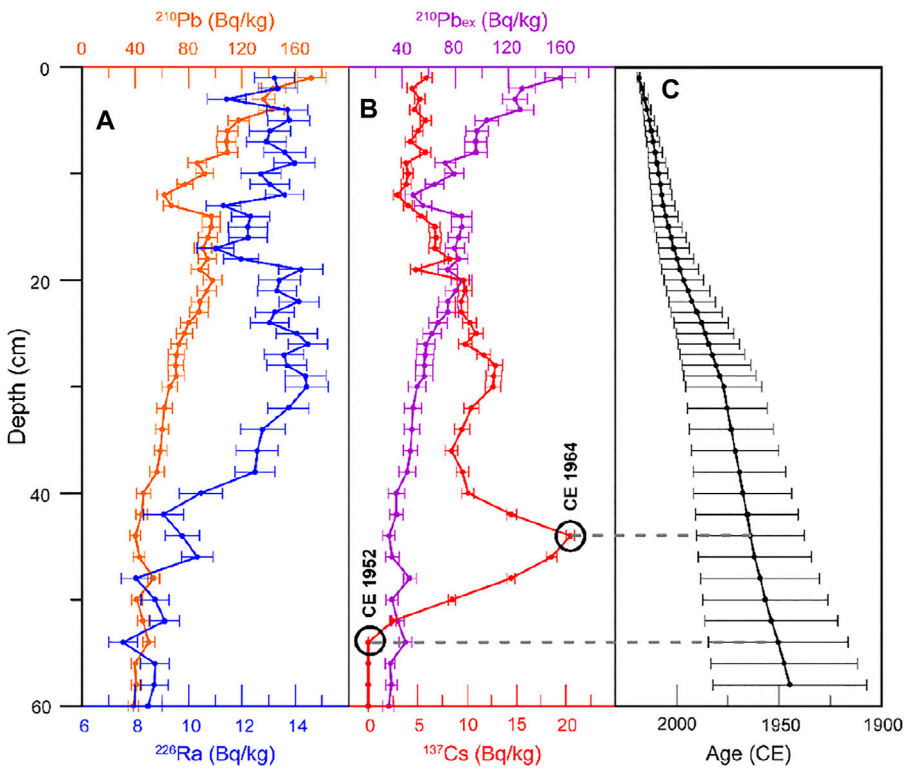

FIGURE 2 | Age–depth model for DH20B based on radionuclide dating results. **(A)** Stratigraphic plots of ^{210}Pb and ^{226}Ra in becquerels per kilogram (Bq/kg) dried sediment. **(B)** Stratigraphic plots of ^{210}Pb$_{ex}$ and ^{137}Cs in Bq/kg dried sediment. **(C)** Age model for DH20B is based on the CRS model (Appleby, 2001).

351.9 keV) and ^{214}Bi (609.3 keV). The excess ^{210}Pb ($^{210}Pb_{ex}$) was calculated with the difference between the activities of ^{210}Pb and ^{226}Ra, which was used to assess the average sedimentation rates. The age–depth model of DH20B was calculated using the constant rate of supply (CRS) model (Appleby, 2001). The dating analysis was carried out at the Key Laboratory of Western China's Environmental Systems, Lanzhou University.

3.3 Analysis of *n*-Alkanes

The subsamples were freeze-dried and homogenized, then ultrasonically extracted in dichloromethane: methanol (v:v = 9: 1) for 15 min (4×). The combined extracts were concentrated to dryness and saponified with 1 N KOH in 95:5 (methanol: H_2O, v: v) for 12 h and extracted with hexane (3×) after quenching the reaction with 5% NaCl solution. The neutral lipids containing *n*-alkanes were further extracted with silica gel column chromatography using hexane. *n*-Alkanes were measured using an Agilent 8,890 gas chromatography (GC) unit equipped with a flame ionization detector (FID) and a split-injector, DB-5 GC column (30 m × 0.32 mm × 0.25 μm), with an external C_8-C_{30} standard (50 ng/μl) for quantification. The detailed oven program was as follows: hold at 40°C for 1 min, heat to 150°C at 10°C/min, ramp (heat) to 310°C at 6°C/min, and hold at 310°C for 10 min. The analyses were carried out in the Key Laboratory of Western China's Environmental Systems, Lanzhou University.

We applied several indexes to present our *n*-alkane results in this study. The concentration percentage of short-, mid-, and long-chain *n*-alkanes to total *n*-alkanes (percentage of x-chain) is defined as formula (*1*). ACL is defined as formula (*2*). The carbon preference index (CPI) is defined as formula (*3*) (Naafs et al., 2019).

$$\textbf{Percentage of x-chain } n\textbf{-alkanes} = \frac{\sum_a^b (C_n)}{\sum_{16}^{35} (C_n)}, \quad (1)$$

$$\textbf{ACL}_{27\text{-}35} = \frac{\sum_{27}^{35} (\mathrm{n} \times \mathrm{C_n})}{\sum_{27}^{35} (\mathrm{C_n})}, \quad (2)$$

$$\textbf{CPI} = \frac{1}{2}\left[\left(\frac{C_{25}+C_{27}+C_{29}+C_{31}+C_{33}}{C_{24}+C_{26}+C_{28}+C_{30}+C_{32}}\right) + \left(\frac{C_{25}+C_{27}+C_{29}+C_{31}+C_{33}}{C_{26}+C_{28}+C_{30}+C_{32}+C_{34}}\right)\right]. \quad (3)$$

In these formulas, n and C_n are the carbon number and the concentration of each *n*-alkane, and x-chain *n*-alkanes represent one of the short-chain, mid-chain, and long-chain *n*-alkanes, with carbon numbers of 16–20, 21–26, and 27–35, respectively.

4 RESULTS

4.1 Dating Results of DH20B

The depth profiles of ^{210}Pb, $^{210}Pb_{ex}$, ^{137}Cs, and ^{226}Ra for DH20B are presented in **Figure 2**. There was a generally decreasing trend of ^{210}Pb (**Figure 2A**) and $^{210}Pb_{ex}$ (**Figure 2B**) activity in DH20B from the top (171.99 and 158.77 Bq/kg) to the bottom (38.47 and 30.00 Bq/kg), and they all reached the background levels. The peak of ^{137}Cs was at the depth of 44 cm, indicating its age was around 1963–1964, because of atmospheric and underwater nuclear weapon testing (**Figure 2B**). Meanwhile, the zero ^{137}Cs at 54 cm represented the onset of large-scale nuclear weapons testing in 1952 (**Figure 2B**). The CRS model (Appleby, 2001) based on $^{210}Pb_{ex}$ activities showed the age of 44 and 54 cm to be 1964.13 and 1950.53, respectively, corresponding to the ^{137}Cs activity results. Overall, DH20B covered at least the last 60 years, from 1960 to 2020 (**Figure 2C**).

4.2 The Concentration and Distribution of *n*-Alkanes

We analyzed C_{16}-C_{35} *n*-alkanes for all samples (**Supplementary Table S1**), with concentrations from 0.01 to 200 μg/g (dry weight). All samples had the odd-to-even carbon preference for mid- and long-chain *n*-alkane concentrations (**Figure 3**). The ∑alk of aquatic and terrestrial plant leaves were 70.33 and 164.64 μg/g, respectively. There was a double-peak pattern of *n*-alkanes in aquatic plant leaf samples (with the peaks of C_{23} and C_{31} *n*-alkane; **Figures 3A**) and a single-peak pattern in terrestrial plant leaf samples (with the peak of C_{31} *n*-alkane; **Figure 3B**). Plant leaf samples all had a very low percentage of short-chain *n*-alkanes, at 1.3% (aquatic plant leaves) and 0.3% (terrestrial plant leaves) (**Figure 4A**). For the mid- and long-chain *n*-alkanes, aquatic plant leaves had a higher percentage of mid-chain *n*-alkanes (24.3% for aquatic plants and 3.9% for terrestrial plants; **Figure 4B**) and terrestrial plant leaves had a higher percentage of long-chain *n*-alkanes (95.7% for terrestrial plants and 71.6% for aquatic plants; **Figure 4C**). In addition, the average $ACL_{27–35}$ value of terrestrial plant leaf samples was larger than that of aquatic plant leaf samples (29.80 vs. 28.03; **Figure 4D**).

The soil and lake sediment samples had a lower ∑alk than plant leaf samples. The average ∑alk results for BSS, LSS, and DH20B samples were 3.13, 2.52, and 1.49 μg/g (**Figures 3C-E**), respectively. The distributions of *n*-alkanes for these samples were similar, with all exhibiting a single-peak pattern of *n*-alkanes (a typical sample with the peak of C_{31} is shown in **Supplementary Figure S1**). For both BSS and LSS samples, the percentages of different chain length *n*-alkanes were generally similar, at about 4.0%, 17.0%, and 79.0% for short-, mid-, and long-chain *n*-alkanes, respectively (**Figure 4**). For DH20B samples, the percentage of short-chain *n*-alkanes was nearly 3–5 times higher than BSS and LSS samples (13.8%; **Figure 4A**), and the percentage of long-chain *n*-alkanes was lower (65.5%; **Figure 4C**). The $ACL_{27–35}$ values of BSS, LSS, and DH20B samples were 29.80, 29.79, and 29.76, respectively (**Figure 4D**).

5 DISCUSSION

5.1 Sources of *n*-Alkanes in Daihai Lake Sediments

The *n*-alkanes can be roughly divided into two groups: biogenic *n*-alkanes (e.g., plant leaf, phytoplankton, and bacteria, etc.) and anthropogenic *n*-alkanes (e.g., vehicle exhaust, petroleum pollution, and organic fuel combustion) (He et al., 2020). Given that there are now intense human activities in the

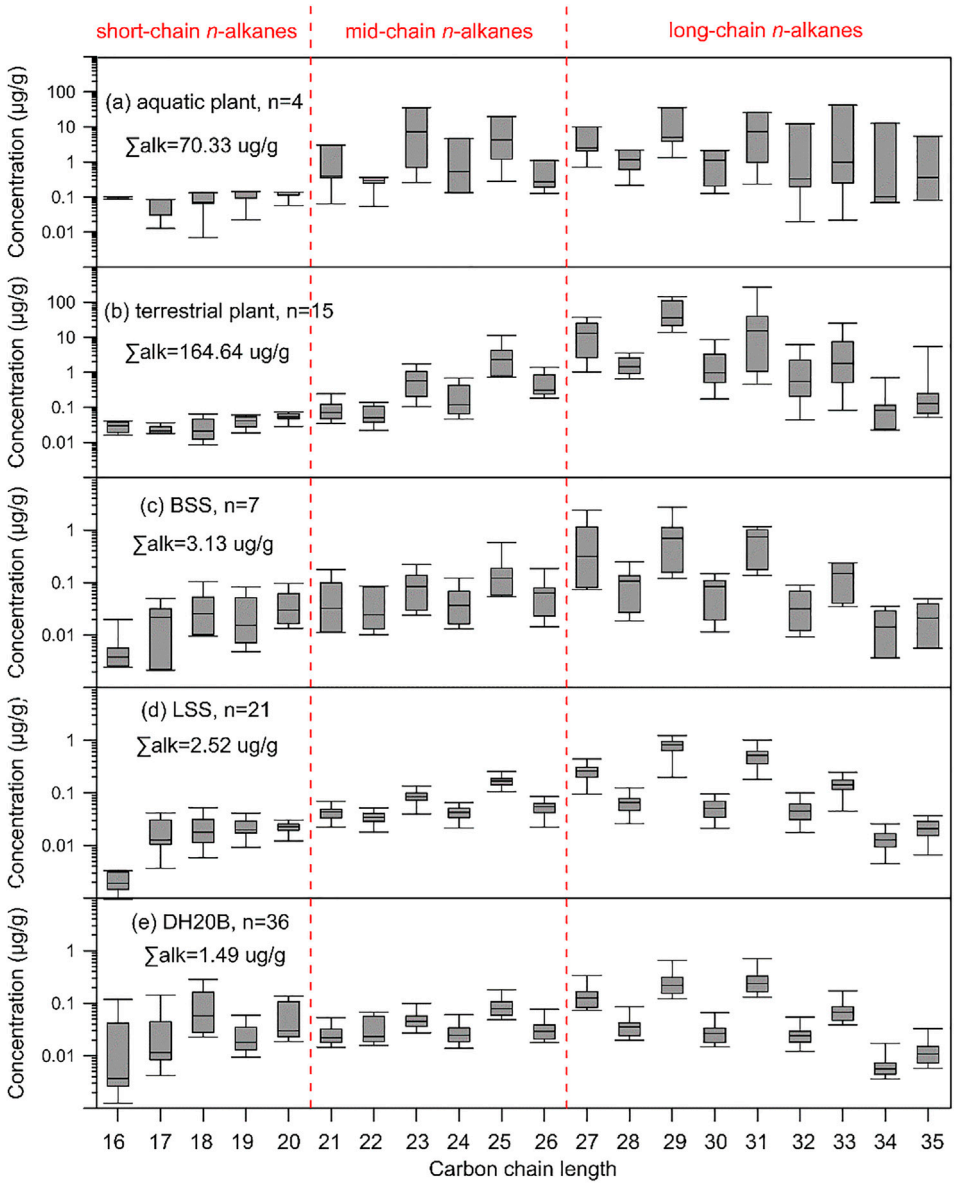

FIGURE 3 | Box-plots of *n*-alkane concentrations from different samples in the Daihai Lake basin. **(A)** Aquatic plant leaf; **(B)** terrestrial plant leaf; **(C)** BSS; **(D)** LSS; and **(E)** DH20B sediment. The *y*-axes are logarithmic coordinates.

Daihai Lake basin, it is necessary first to investigate the formation pathway of the *n*-alkanes. It has been proved that biogenic *n*-alkanes have a significant odd carbon preference, but that anthropogenic *n*-alkanes do not have such a pattern (Simoneit, 1989; He et al., 2020). Thus, the carbon preference index (CPI) is designed to evaluate the contribution of biogenic and anthropogenic *n*-alkanes. When CPI >3, it is thought that the *n*-alkanes are dominated by biogenic sources (Simoneit, 1989). We calculated CPI for all the lake sediment samples and found them all to be larger than 3 (**Supplementary Figure S2**), confirming their biogenic sources.

The sources of biogenic *n*-alkanes in the lake can be roughly divided into two parts: allochthonous sources (e.g., basin soils) and autochthonous sources (e.g., aquatic plants and algae). Many researchers have pointed out that there are significant discrepancies in different chain length *n*-alkanes between these two sources (Volkman et al., 1999; Castañeda and Schouten, 2011; Bush and McInerney, 2013; Naafs et al., 2019; Kou et al., 2020). For example, terrestrial plants preferentially synthesize long-chain *n*-alkanes, and aquatic plants produce a higher percentage of mid-chain *n*-alkanes. Our modern leaf results (**Figure 4**) indicated that 95.7% of *n*-alkanes produced by terrestrial plants belonged to long-chain *n*-alkanes and only 3.9% to mid-chain *n*-alkanes. But for aquatic plants, the percentage of mid-chain *n*-alkanes reached 24.3%, and the percentage of long-chain *n*-alkanes was 71.6%. Thus, based on

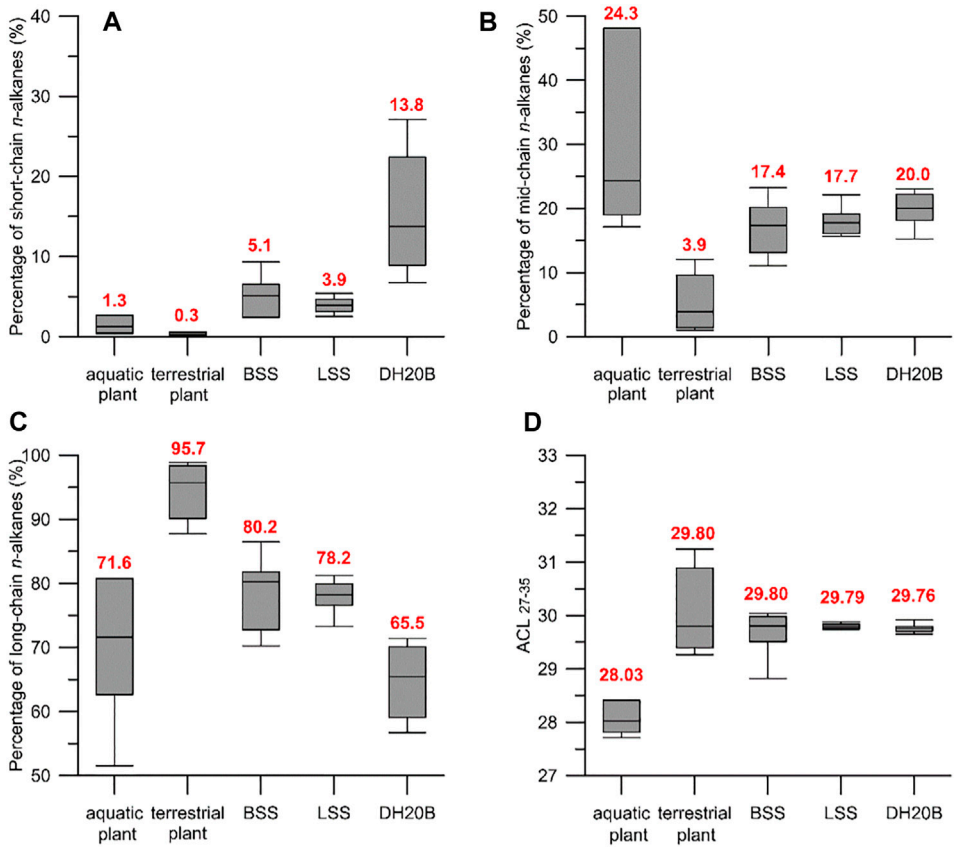

FIGURE 4 | Percentage of different chain length *n*-alkanes and ACL results from different samples. **(A)** Percentage of short-chain *n*-alkanes; **(B)** percentage of mid-chain *n*-alkanes; **(C)** percentage of long-chain *n*-alkanes; and **(D)** ACL of *n*-alkanes with carbon numbers from 27 to 35.

the percentage of different chain-length *n*-alkanes, it might be possible to distinguish the sources of *n*-alkanes in Daihai Lake sediments. However, it should be noted that it was more reasonable to have used BSS as the allochthonous source of *n*-alkanes in the lake sediment, rather than terrestrial plants, since these were the direct inputs of allochthonous *n*-alkanes.

For the LSS samples, the percentages of short-, mid-, and long-chain *n*-alkanes were generally the same as the BSS samples (**Figure 4**), with about 4.0%, 17.0%, and 79.0%, respectively. This similar distribution indicated that the *n*-alkanes in LSS were dominated by allochthonous sources. For the DH20B samples, the percentage of mid-chain *n*-alkanes was generally the same as for BSS (20.0% vs. 17.4%). The most obvious difference between them was the percentage of short-chain *n*-alkanes (13.8% vs. 5.1%). To analyze the causes, the percentage of short-chain *n*-alkanes of DH20B is presented in **Supplementary Figure S3**, which shows the percentage was ~9% (near BSS) before 2008 but ~25% (much higher than BSS) between 2008 and 2018. We speculate that this significant change can be attributed to the Daihai power plant (built in 2005): the power plant used large volumes of lake water to cool the facility after 2008, and then the warmed water was directly poured into Daihai Lake (Inner Mongolia Water Conservancy and Hydropower Survey and Design Institute, 2015). This process would change both the nutritional status and lake water temperature. Many previous researchers have proposed that nutritional status is the main factor leading to the outbreak of algae, such as in Yanghe Reservoir (Wang et al., 2013) and Taihu Lake (Duan et al., 2009). In addition, the cooling water was specific to Daihai Lake compared with other sites, which could also significantly increase water temperature and induce algae bloom (Chen et al., 2018). Thus, we propose that nutritional status and water temperature induced by cooling water were the main factors leading to the outbreak of algae (leading to more short-chain *n*-alkanes) in Daihai Lake. After 2018, alongside the disuse of cooling water, the percentage of short-chain *n*-alkanes returned to a low level (**Supplementary Figure S3**). Thus, except between 2008 and 2018, the characteristics of DH20B sediments were also similar to those of BSS, which implied that *n*-alkanes in DH20B were mainly derived from allochthonous sources. In addition, ACL_{27-35} values of lake sediments (29.79 for LSS and 29.76 for DH20B) were closer to those of BSS (29.80) than to those of aquatic plant leaves (28.03) (**Figure 4D**), which also supported the proposition that *n*-alkanes in Daihai Lake sediments (dominated by long-

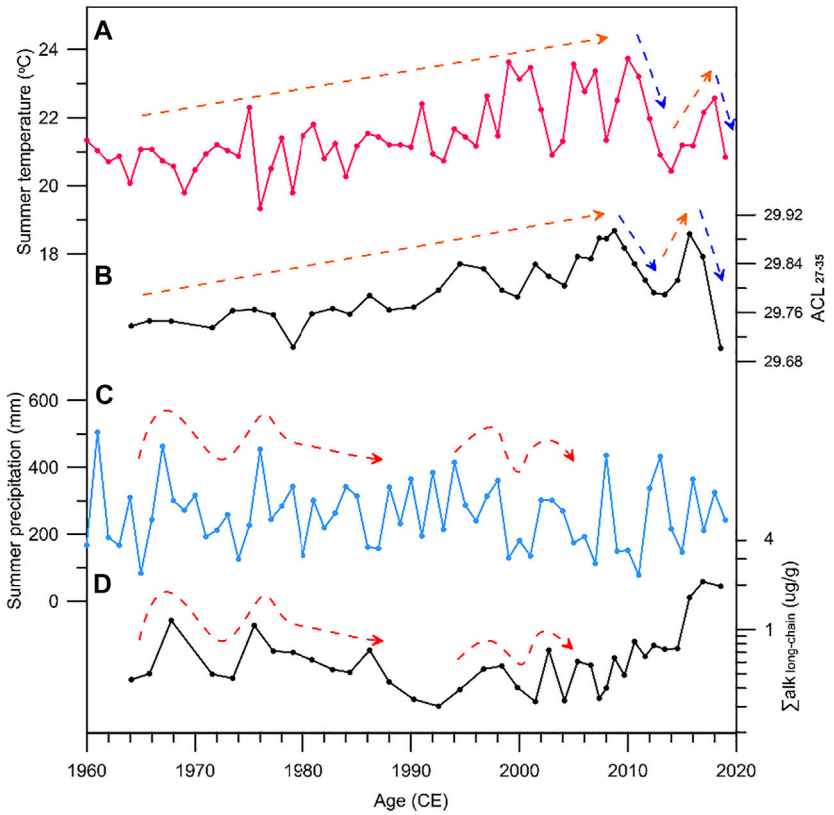

FIGURE 5 | Comparisons of climatic variables and *n*-alkane results over the last 60 years. **(A)** Summer temperature; **(B)** ACL_{27-35} record; **(C)** summer precipitation; and **(D)** $\sum alk_{long\text{-}chain}$ record (the *y*-axis is a logarithmic coordinate). Meteorological data are from the Hohhot Weather Station (www.cma.gov.cn).

chain *n*-alkanes) were mainly derived from allochthonous sources.

5.2 Implications for Paleoclimate Reconstruction

5.2.1 Paleoclimatic Interpretation of ACL

Interpretation of ACL in lake sediments can be roughly divided into the following two aspects: 1) temperature. Normally, a higher temperature can make higher plants synthesize longer chain compounds to preserve more water from intense plant transpiration (Xie et al., 2003; Castañeda and Schouten, 2011). A core premise of this mechanism is that the source of *n*-alkanes should be allochthonous (e.g., terrestrial plants) (Sikes et al., 2009). This hypothesis was supported by paleoclimate research in northern China, such as at Xijianhaizi Lake (Dong et al., 2022). 2) Vegetation type. Sun et al. (2013) found that aquatic plants produced non-negligible quantities of *n*-alkanes in Xiaolongwan Lake and significantly influenced the ACL proxy, and thus ACL can partly indicate the autochthonous inputs. Evidence from Tianchi Lake (Sun et al., 2018) and Dabusu Lake (Sawada et al., 2020) in northern China also pointed out that mid-chain *n*-alkanes produced by aquatic plants strongly affected ACL.

In Daihai Lake, based on the similar distributions of *n*-alkanes between BSS, LSS, and DH20B, we suggested that *n*-alkanes in Daihai Lake were dominated by allochthonous sources, which was also supported by other case studies such as Beilianchi Lake (Zhang et al., 2020) and Lugu Lake (Zhao et al., 2021). Meanwhile, only the long-chain *n*-alkanes (C_{27}–C_{35}) were chosen to calculate the ACL, excluding the influence of the mid-chain *n*-alkanes by aquatic plants (Volkman et al., 1999; Bush and McInerney, 2013). In addition, ACL_{27-35} of our LSS samples was 29.79, which was very similar to that of modern terrestrial plant leaves (29.80) and was significantly higher than that of aquatic plant leaves (28.03) (**Figure 4D**). These various lines of evidence indicate that the lake sediments recorded the signals of ACL_{27-35} from terrestrial plants, and thus the aquatic plant effect was not obvious in Daihai Lake when we used the ACL_{27-35} proxy. Admittedly, terrestrial plant types can also influence the ACL_{27-35} values (Bush and McInerney, 2013). For example, Diefendorf and Freimuth (2017) pointed out that angiosperms and gymnosperms had different ACL_{27-35} values at the same temperature, although they are all C_3 woody plants. Nevertheless, we found the time series of ACL_{27-35} recorded by DH20B had a similar variation with regional summer temperature over the last 60 years (**Figure 5**). These had a significant correlation coefficient of 0.54 ($p < 0.01$; **Figure 6A**). In Daihai Lake, this positive correlation between ACL_{27-35} and summer temperature

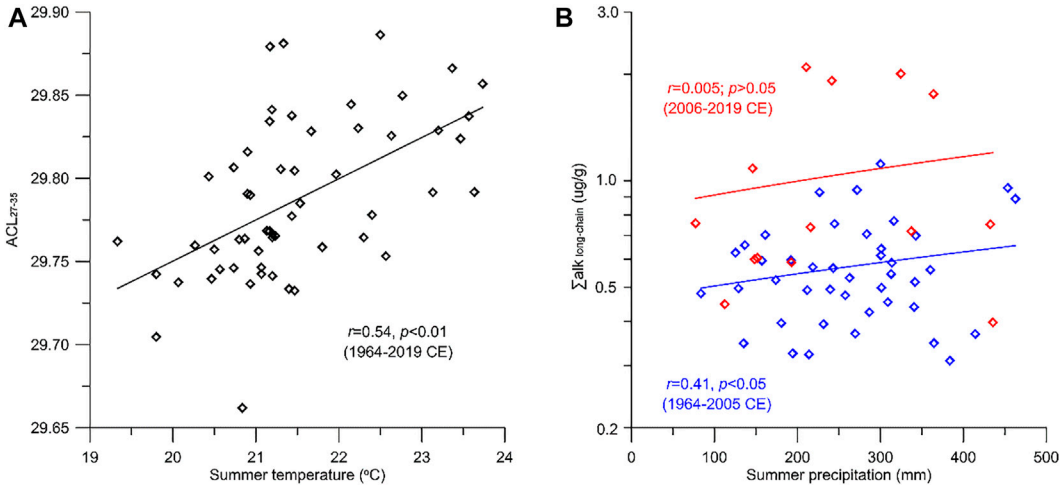

FIGURE 6 | Correlation coefficient results. **(A)** Summer temperature and $ACL_{27–35}$; **(B)** summer precipitation and $\sum alk_{long\text{-}chain}$.

supported the view of temperature-controlled ACL (Sikes et al., 2009; Wang et al., 2018; Naafs et al., 2019).

5.2.2 Paleoclimatic Interpretation of $\sum alk_{long\text{-}chain}$

∑alk is a proxy to indicate regional biomass and productivity, which are normally linked to vegetation coverage (Zhang et al., 2019). Precipitation and temperature are two main factors influencing this proxy (Wang et al., 2018; Shi et al., 2021). On the one hand, abundant precipitation can promote the growth of plants (Chen et al., 2015). Thus, there would be more biosynthetic *n*-alkanes due to the flourishing development of vegetation (Zhang et al., 2019; Shi et al., 2021). On the other hand, the temperature can also influence plant growth. As temperature increases (within physiological range), most plant processes (e.g., photosynthesis, transpiration, and respiration) can all intensify. This would also promote the production of *n*-alkanes by plants (Wang et al., 2018; Sun et al., 2019).

We found $\sum alk_{long\text{-}chain}$ had a positive correlation with summer precipitation ($r = 0.41$, $p < 0.05$; **Figure 6B**) except for the period after 2005, and it was not correlated with temperature ($r = 0.08$, $p > 0.05$; **Supplementary Figure S4**). The reason we used long-chain *n*-alkanes to calculate ∑alk is that long-chain *n*-alkanes can better represent the change of terrestrial vegetation in Daihai Lake. The high correlation between $\sum alk_{long\text{-}chain}$ and summer precipitation indicated that $\sum alk_{long\text{-}chain}$ in Daihai Lake is a proxy of summer precipitation. Previous studies also demonstrated that precipitation is the major limiting factor influencing plant growth in the Daihai Lake basin (e.g., Jin et al., 2013; Xiao et al., 2019). But in some other lakes, such as Xingkai Lake—which is further north than Daihai Lake—temperature seems to be the dominant factor, rather than precipitation, because of the influence of the short growing season and low annual temperature (Sun et al., 2019). One special issue to note is that, after 2005, $\sum alk_{long\text{-}chain}$ gradually increased, but summer precipitation did not follow such a trend (**Figure 5**). The poor correlation between them ($r = 0.005$, $p > 0.05$; **Figure 6B**) also demonstrated this. Obviously, some other factors influenced the changes in $\sum alk_{long\text{-}chain}$ in Daihai Lake after 2005.

5.3 Human Impacts on *n*-Alkanes in Daihai Lake Sediment

Human activity can strongly influence *n*-alkanes in lake sediments (He et al., 2020). To evaluate the potential effects of such activity, the population in the Daihai Lake basin (Liang et al., 2017) and livestock production in Liangcheng County (10 km from Daihai Lake, Sun et al., 2021) were used in this study. The results showed that regional human activity was relatively weak before 1996, gradually intensified after 1996, and reached a peak after 2005 (**Figure 7**). Notably, the Daihai Lake power plant was built in 2005 (Inner Mongolia Water Conservancy and Hydropower Survey and Design Institute, 2015). In order to use the lake water to cool the power generation units, an artificial channel was excavated. Evidently, human activity in the Daihai Lake basin had strengthened significantly after 2005.

As discussed in the aforementioned section, neither precipitation nor temperature can explain the changes of $\sum alk_{long\text{-}chain}$ after 2005. Interestingly, we found the timings of increased $\sum alk_{long\text{-}chain}$ (**Figure 7D**) and intensified human activity (**Figures 7A,B**) were nearly synchronous. Thus, we speculated that human activity is the reason for the increased $\sum alk_{long\text{-}chain}$: intensified human activity increased regional biomass through large areas of crops and pastures (Liang et al., 2017; Sun et al., 2021), and then basin soils with a high concentration of long-chain *n*-alkanes were transported into the lake through seasonal inflows and the artificial channel. Meanwhile, both $\sum alk_{mid\text{-}chain}$ and $\sum alk_{short\text{-}chain}$ were found to have increased after 2005 (**Figure 7D**) because of the flourishing of aquatic plants (mid-chain *n*-alkanes) and the outbreak of algae (short-chain *n*-alkanes) due to changes in nutritional status and warming of water caused by intense human activities. Additionally, it was noted that human activity had a gradually increasing trend from 1996 to 2005, but that $\sum alk_{long\text{-}chain}$ did not

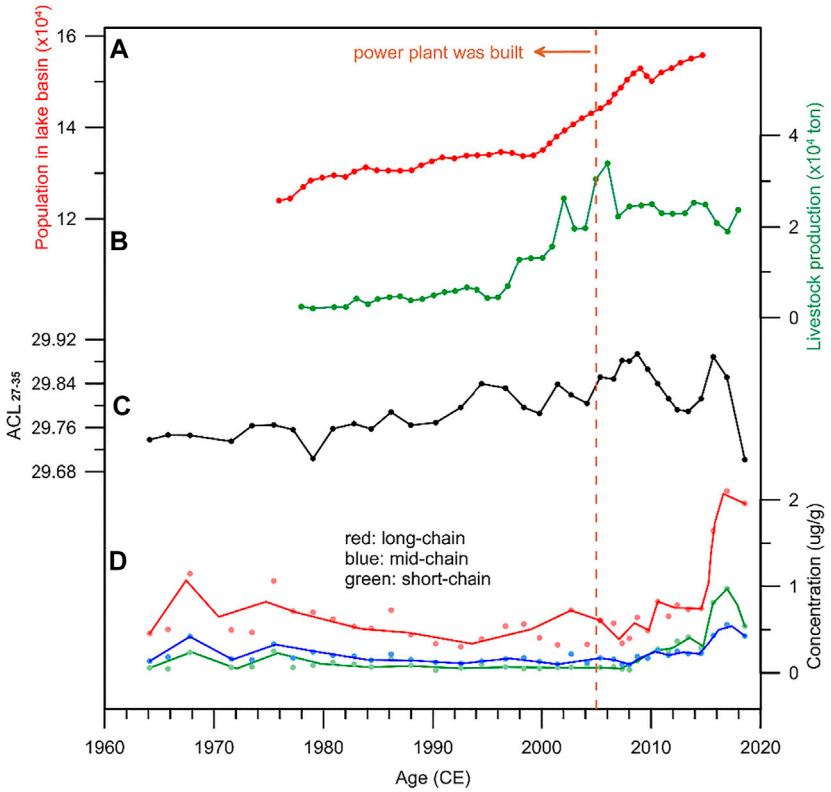

FIGURE 7 | Human impacts on *n*-alkanes in Daihai Lake over the last 60 years. **(A)** Population in the Daihai Lake basin (Liang et al., 2017). **(B)** Livestock production in Liangcheng County (Sun et al., 2021). **(C)** $ACL_{27–35}$ record of DH20B. **(D)** *n*-Alkane concentration of DH20B: red, long-chain *n*-alkanes; blue, mid-chain *n*-alkanes; and green, short-chain *n*-alkanes. The curves were fitted by spline smoothing (with five points).

show similar variations (**Figure 7**). It can be speculated that the overall decreased summer precipitation may have obscured the signals of human activity (**Figure 5C**).

However, unlike $\sum alk_{long\text{-}chain}$, $ACL_{27–35}$ seems not to have been influenced by intense human activity after 2005 (**Figure 7C**) and has been maintaining a good correlation with summer temperature since 1964 (**Figure 6A**). This is because, for each individual compound (C_{27}, C_{29}, C_{31}, C_{33}, and C_{35}) of long-chain *n*-alkanes, human activity cannot further alter the proportion through farming and grazing, and only biochemical processes (such as the decarboxylation pathway) in living organisms can have influence (Sikes et al., 2009; Castañeda and Schouten, 2011; Villanueva et al., 2014), i.e., to reduce the transpiration of plant leaves in higher temperature conditions, terrestrial plants are more likely to synthesize longer *n*-alkanes in leaf cells. Based on the computational formula (Naafs et al., 2019), $ACL_{27–35}$ is only influenced by the proportion of different individual compounds of long-chain *n*-alkanes and thus is less influenced by human activity.

In conclusion, human activity can greatly influence ∑alk and has little effect on $ACL_{27–35}$. For this reason, care must be taken when using ∑alk in paleoclimate reconstruction, especially during a period with intense human activity, such as the late Holocene. Given that our records only cover 60 years, it is inevitable that some additional factors (e.g., degradation, deposition processes, and wildfire impacts) in the past would also have influenced the *n*-alkanes in the lake sediment, and thus more proxy validation studies are needed in the future.

6 CONCLUSION

A proxy validation study of *n*-alkanes in the Daihai Lake basin was carried out to investigate the implications for the interpretation of paleoclimate research. Our conclusions are as follows:

1) In Daihai Lake, the percentages of different chain *n*-alkanes in lake sediments were similar to those in the basin soil, which indicated that the *n*-alkanes were mainly derived from allochthonous sources. It should be noted, however, that the short-chain *n*-alkanes dramatically increased in the period ~2008–2018. This is because warm water produced by the Daihai power plant promoted the growth of algae.
2) Based on the results of the DH20B sediment core, we found that $ACL_{27–35}$ and $\sum alk_{long\text{-}chain}$ were correlated with regional summer temperature and summer precipitation over the last 60 years, except when $\sum alk_{long\text{-}chain}$ was

affected by human activity after 2005. Thus, we propose that ACL_{27-35} and $\sum alk_{long\text{-}chain}$ in Daihai Lake are suitable proxies to represent summer temperature and summer precipitation, respectively. The reasons are that higher summer temperature promotes the synthesis of longer *n*-alkanes to reduce water loss (higher ACL_{27-35}), and increased summer precipitation promotes plant growth and more *n*-alkanes can be synthesized (higher $\sum alk_{long\text{-}chain}$). Our findings may have broad significance for paleoclimate reconstruction in other hydrologically closed lakes which are similar to Daihai Lake.

3) Since 2005, intense human activity dramatically has been increasing $\sum alk_{long\text{-}chain}$ in Daihai Lake through cultivation and grazing, but it did not have obvious effects on ACL_{27-35}. Thus, human activity has to be considered if $\sum alk_{long\text{-}chain}$ is used in paleoclimate research. Given that our records only extended 60 years, some other contributing factors (e.g., degradation, deposition processes, and wildfire impacts) were not considered; thus further research is needed in the future.

DATA AVAILABILITY STATEMENT

The original contributions presented in the study are included in the article/**Supplementary Material**; further inquiries can be directed to the corresponding authors.

AUTHOR CONTRIBUTIONS

ZS: writing, data analysis, and laboratory work. ZZ: writing and data analysis. JC: laboratory work and investigation. LC: laboratory work and investigation. XP: investigation. RC: investigation. JL: methodology and funding acquisition. SC: writing and data analysis.

FUNDING

This work was supported by the National Natural Science Foundation of China (awards 42071115 and 41790421).

ACKNOWLEDGMENTS

We sincerely thank Xianyu Huang, Yanwu Duan, and Wengang Kang, who provided helpful suggestions, and Yuanxin Li, who helped with experimental works.

SUPPLEMENTARY MATERIAL

The Supplementary Material for this article can be found online at: https://www.frontiersin.org/articles/10.3389/feart.2022.915500/full#supplementary-material

REFERENCES

Appleby, P. G. (2001). "Basin Analysis, Coring, and Chronological Techniques," in *Tracking Environmental Change Using Lake Sediments-Volume 1*. Editors W. M. Last and J. P. Smol (Netherlands: Springer), 171–203.

Bush, R. T., and McInerney, F. A. (2013). Leaf Wax *n*-Alkane Distributions in and across Modern Plants: Implications for Paleoecology and Chemotaxonomy. *Geochimica Cosmochimica Acta* 117, 161–179. doi:10.1016/j.gca.2013.04.016

Castañeda, I. S., and Schouten, S. (2011). A Review of Molecular Organic Proxies for Examining Modern and Ancient Lacustrine Environments. *Quat. Sci. Rev.* 30, 2851–2891. doi:10.1016/j.quascirev.2011.07.009

Chen, F., Xu, Q., Chen, J., Birks, H. J., Liu, J., Zhang, S., et al. (2015). East Asian Summer Monsoon Precipitation Variability Since the Last Deglaciation. *Sci. Rep.* 5, 11186. doi:10.1038/srep11186

Chen, J., Liu, J., Xie, C., Chen, G., Chen, J., Zhang, Z., et al. (2018). Biogeochemical Responses to Climate Change and Anthropogenic Nitrogen Deposition from a ~200-Year Record from Tianchi Lake, Chinese Loess Plateau. *Quat. Int.* 493, 22–30. doi:10.1016/j.quaint.2018.09.004

Diefendorf, A. F., and Freimuth, E. J. (2017). Extracting the Most from Terrestrial Plant-Derived n-Alkyl Lipids and Their Carbon Isotopes from the Sedimentary Record: A Review. *Org. Geochem.* 103, 1–21. doi:10.1016/j.orggeochem.2016.10.016

Dong, H., Xie, M., Shang, W., Liu, S., Ling, Y., Zhan, N., et al. (2022). Plant-Wax Carbon Isotopic Evidence of Lateglacial and Holocene Climate Change from Lake Sediments in the Yin Mountains, Inner Mongolia. *Quat. Int.* 622, 10–20. doi:10.1016/j.quaint.2021.12.017

Duan, H., Ma, R., Xu, X., Kong, F., Zhang, S., Kong, W., et al. (2009). Two-Decade Reconstruction of Algal Blooms in China's Lake Taihu. *Environ. Sci. Technol.* 43, 3522–3528. doi:10.1021/es8031852

Duan, Y., Wu, Y., Cao, X., Zhao, Y., and Ma, L. (2014). Hydrogen Isotope Ratios of Individual n-Alkanes in Plants from Gannan Gahai Lake (China) and Surrounding Area. *Org. Geochem.* 77, 96–105. doi:10.1016/j.orggeochem.2014.10.005

Duan, Y., and Xu, L. (2012). Distributions of *n*-Alkanes and Their Hydrogen Isotopic Composition in Plants from Lake Qinghai (China) and the Surrounding Area. *Appl. Geochem.* 27, 806–814. doi:10.1016/j.apgeochem.2011.12.008

Eglinton, G., and Hamilton, R. J. (1967). Leaf Epicuticular Waxes: The Waxy Outer Surfaces of Most Plants Display a Wide Diversity of Fine Structure and Chemical Constituents. *Science* 156, 1322–1335. doi:10.1126/science.156.3780.1322

Ficken, K. J., Li, B., Swain, D. L., and Eglinton, G. (2000). An *n*-Alkane Proxy for the Sedimentary Input of Submerged/Floating Freshwater Aquatic Macrophytes. *Org. Geochem.* 31, 745–749. doi:10.1016/s0146-6380(00)00081-4

He, Y., Yang, C., He, W., Liu, W., and Xu, F. (2020). New Insights into Spatiotemporal Source Apportionment of *n*-Alkanes under Mixed Scenario: A Pilot Study on Lake Chaohu, China. *Sci. Total Environ.* 742, 140517. doi:10.1016/j.scitotenv.2020.140517

Huang, X., Zhao, B., Wang, K., Hu, Y., and Meyers, P. A. (2018). Seasonal Variations of Leaf Wax *n*-Alkane Molecular Composition and δD Values in Two Subtropical Deciduous Tree Species: Results from a Three-Year Monitoring Program in Central China. *Org. Geochem.* 118, 15–26. doi:10.1016/j.orggeochem.2018.01.009

Inner Mongolia Water Conservancy and Hydropower Survey and Design Institute (2015). Project for Water Ecological Protection in Daihai Lake. *Ulanchab*, 1–46.

Jin, Z., Li, X., Zhang, B., Han, Y., and Zheng, G. (2013). Geochemical Records in Holocene Lake Sediments of Northern China: Implication for Natural and Anthropogenic Inputs. *Quat. Int.* 304, 200–208. doi:10.1016/j.quaint.2013.04.019

Kou, Q., Lin, X., Wang, J., Yu, S., Kai, J., Laug, A., et al. (2020). Spatial Distribution of n-Alkanes in Surface Sediments of Selin Co Lake, Central Tibetan Plateau, China. *J. Paleolimnol.* 65, 53–67. doi:10.1007/s10933-020-00148-8

Liang, W. J., Chun, X., Liu, J. Y., Xue, M., Siqin, B. L. G., Wu, Z. W., et al. (2017). Research on the Area Change Processes in the Past 40a of Daihai Lake. *J. Arid Land Resour. Environ.* 31, 93–98. doi:10.13448/j.cnki.jalre.2017.116

Liang, X., Liu, H. M., Ji, M. C., Chang, M., Wen, L., Yu, R. H., et al. (2021). Effects of Land Use/Cover Change on Lake Water Quality in the Semi-Arid Region of

Northern China: A Case Study in Lake Daihai Basin (2000-2018). *J. Lake Sci.* 33, 727–736. doi:10.18307/2021.0309

Naafs, B. D. A., Inglis, G. N., Blewett, J., McClymont, E. L., Lauretano, V., Xie, S., et al. (2019). The Potential of Biomarker Proxies to Trace Climate, Vegetation, and Biogeochemical Processes in Peat: A Review. *Glob. Planet. Change* 179, 57–79. doi:10.1016/j.gloplacha.2019.05.006

Sawada, K., Ono, M., Nakamura, H., and Tareq, S. M. (2020). Reconstruction of Holocene Optimum Paleoclimatic Variations Using Long-Chain *n*-Alkanes and Alkenones in Sediments from Dabusu Lake, Northeastern China. *Quat. Int.* 550, 27–38. doi:10.1016/j.quaint.2020.03.011

Shen, Z., Liu, J., Xie, C., Zhang, X., and Chen, F. (2018). An Environmental Perturbation at AD 600 and Subsequent Human Impacts Recorded by Multi-Proxy Records from the Sediments of Lake Mayinghai, North China. *Holocene* 28, 1870–1880. doi:10.1177/0959683618798159

Shi, M., Han, J., Wang, G., Wang, J., Han, Y., and Cui, L. (2021). A Long-Term Investigation of the Variation in Leaf Wax n-Alkanes Responding to Climate on Dongling Mountain, North China. *Quat. Int.* 592, 67–79. doi:10.1016/j.quaint.2021.04.020

Sikes, E. L., Uhle, M. E., Nodder, S. D., and Howard, M. E. (2009). Sources of Organic Matter in a Coastal Marine Environment: Evidence from *n*–Alkanes and Their $\delta^{13}C$ Distributions in the Hauraki Gulf, New Zealand. *Mar. Chem.* 113, 149–163. doi:10.1016/j.marchem.2008.12.003

Simoneit, B. R. T. (1989). Organic–matter of the Troposphere–V: Application of Molecular Marker Analysis to Biogenic Emissions into the Troposphere for Source Reconciliations. *J. Atmos. Chem.* 8, 251–275. doi:10.1007/bf00051497

Sun, H., Bendle, J., Seki, O., and Zhou, A. (2018). Mid-to-Late Holocene Hydroclimatic Changes on the Chinese Loess Plateau: Evidence from N-Alkanes from the Sediments of Tianchi Lake. *J. Paleolimnol.* 60, 511–523. doi:10.1007/s10933-018-0037-9

Sun, Q., Xie, M., Shi, L., Zhang, Z., Lin, Y., Shang, W., et al. (2013). Alkanes, Compound-Specific Carbon Isotope Measures and Climate Variation during the Last Millennium from Varved Sediments of Lake Xiaolongwan, Northeast China. *J. Paleolimnol.* 50, 331–344. doi:10.1007/s10933-013-9728-4

Sun, W., Ni, Z., Meng, X., Jiang, Q., and Zhang, E. (2021). Environmental Change Recorded by Radionuclides and Organic Geochemical Signatures in a Sediment Core from Lake Daihai, North China. *CATENA* 206, 105564. doi:10.1016/j.catena.2021.105564

Sun, W., Zhang, E., Chen, R., and Shen, J. (2019). Lacustrine Carbon Cycling Since the Last Interglaciation in Northeast China: Evidence from *n*-Alkanes in the Sediments of Lake Xingkai. *Quat. Int.* 523, 101–108. doi:10.1016/j.quaint.2019.07.004

Villanueva, L., Damsté, J. S. S., and Schouten, S. (2014). A Re-Evaluation of the Archaeal Membrane Lipid Biosynthetic Pathway. *Nat. Rev. Microbiol.* 12, 438–448. doi:10.1038/nrmicro3260

Volkman, J. K., Barrett, S. M., and Blackburn, S. I. (1999). Eustigmatophyte Microalgae Are Potential Sources of C_{29} Sterols, C_{22}-C_{28} *N*-Alcohols and C_{28}-C_{32}n-Alkyl Diols in Freshwater Environments. *Org. Geochem.* 30, 307–318. doi:10.1016/s0146-6380(99)00009-1

Wang, J., Axia, E., Xu, Y., Wang, G., Zhou, L., Jia, Y., et al. (2018). Temperature Effect on Abundance and Distribution of Leaf Wax *n*-Alkanes across a Temperature Gradient along the 400 Mm Isohyet in China. *Org. Geochem.* 120, 31–41. doi:10.1016/j.orggeochem.2018.03.009

Wang, L., Liu, L., and Zheng, B. (2013). Eutrophication Development and its Key Regulating Factors in a Water-Supply Reservoir in North China. *J. Environ. Sci.* 25, 962–970. doi:10.1016/s1001-0742(12)60120-x

Wang, S. M., Yu, Y. S., Wu, R. J., and Feng, M. (1990). *The Daihai Lake: Lake Environment and Climate Change*. Hefei: Science and Technology University of China Press, 1–191. (in Chinese).

Xiao, J., Zhang, S., Fan, J., Wen, R., Xu, Q., Inouchi, Y., et al. (2019). The 4.2 Ka Event and its Resulting Cultural Interruption in the Daihai Lake Basin at the East Asian Summer Monsoon Margin. *Quat. Int.* 527, 87–93. doi:10.1016/j.quaint.2018.06.025

Xie, S. C., Liang, B., Guo, J. Q., Yi, Y., Evershed, R. P., Maddy, D., et al. (2003). Biomarkers and the Related Global Changes. *Quat. Sci.* 23, 521–528. doi:10.3321/j.issn:1001-7410.2003.05.007

Zhang, C., Zhao, C., Yu, Z., Zhang, H., Zhou, A., Zhang, X., et al. (2020). Western Pacific Ocean Influences on Monsoon Precipitation in the Southwestern Chinese Loess Plateau Since the Mid-Holocene. *Clim. Dyn.* 54, 3121–3134. doi:10.1007/s00382-020-05159-9

Zhang, C., Zhao, C., Zhou, A., Zhang, K., Wang, R., and Shen, J. (2019). Late Holocene Lacustrine Environmental and Ecological Changes Caused by Anthropogenic Activities in the Chinese Loess Plateau. *Quat. Sci. Rev.* 203, 266–277. doi:10.1016/j.quascirev.2018.11.020

Zhao, C., Cheng, J., Wang, J. J., Yan, H., Leng, C. C., Zhang, C., et al. (2021). Paleoclimate Significance of Reconstructed Rainfall Isotope Changes in Asian Monsoon Region. *Geophys. Res. Lett.* 48, e2021GL092460. doi:10.1029/2021gl092460

Zheng, Y. E., Zhou, L. P., and Zhang, J. F. (2010). Optical Dating of the Upper 22m of Cored Sediments from Daihai Lake, Northern China. *Quat. Geochronol.* 5, 228–232. doi:10.1016/j.quageo.2009.05.010

Zhou, W., Zheng, Y., Meyers, P. A., Jull, A. J. T., and Xie, S. (2010). Postglacial Climate-Change Record in Biomarker Lipid Compositions of the Hani Peat Sequence, Northeastern China. *Earth Planet. Sci. Lett.* 294, 37–46. doi:10.1016/j.epsl.2010.02.035

Conflict of Interest: The authors declare that the research was conducted in the absence of any commercial or financial relationships that could be construed as a potential conflict of interest.

The handling editor (XC) declared a shared affiliation with the author(s) (JL and SC) at the time of review.

Publisher's Note: All claims expressed in this article are solely those of the authors and do not necessarily represent those of their affiliated organizations, or those of the publisher, the editors, and the reviewers. Any product that may be evaluated in this article, or claim that may be made by its manufacturer, is not guaranteed or endorsed by the publisher.

Copyright © 2022 Shen, Zhang, Chen, Chen, Pang, Chen, Liu and Chen. This is an open-access article distributed under the terms of the Creative Commons Attribution License (CC BY). The use, distribution or reproduction in other forums is permitted, provided the original author(s) and the copyright owner(s) are credited and that the original publication in this journal is cited, in accordance with accepted academic practice. No use, distribution or reproduction is permitted which does not comply with these terms.